Studies on the Modification of Commercial Bisphenol-A-Based Epoxy Resin Using Different Multifunctional Epoxy Systems

applied mechanics

MDPI

Article

Studies on the Modification of Commercial Bisphenol-A-Based Epoxy Resin Using Different Multifunctional Epoxy Systems

Ankur Bajpai *, James R. Davidson and Colin Robert

School of Engineering, Institute for Materials and Processes, The University of Edinburgh, King's Buildings, Edinburgh EH9 3FB, UK; j.r.davidson@ed.ac.uk (J.R.D.); colin.robert@ed.ac.uk (C.R.)
* Correspondence: ankur.bajpai@ed.ac.uk

Abstract: The tensile fracture mechanics and thermo-mechanical properties of mixtures composed of two kinds of epoxy resins of different chemical structures and functional groups were studied. The base resin was a bi-functional epoxy resin based on diglycidyl ether of bisphenol-A (DGEBA) and the other resins were (a) distilled triglycidylether of meta-amino phenol (b) 1, 6–naphthalene di epoxy and (c) fluorene di epoxy. This research shows that a small number of multifunctional epoxy systems, both di- and tri-functional, can significantly increase tensile strength (14%) over neat DGEBA while having no negative impact on other mechanical properties including glass transition temperature and elastic modulus. In fact, when compared to unmodified DGEBA, the tri-functional epoxy shows a slight increase (5%) in glass transition temperature at 10 wt.% concentration. The enhanced crosslinking of DGEBA (90 wt.%)/distilled triglycidylether of meta-amino phenol (10 wt.%) blends may be the possible reason for the improved glass transition. Finally, the influence of strain rate, temperature and moisture were investigated for both the neat DGEBA and the best performing modified system. The neat DGEBA was steadily outperformed by its modified counterpart in every condition.

Keywords: epoxy resins; mechanical properties; multifunctional epoxies

Citation: Bajpai, A.; Davidson, J.R.; Robert, C. Studies on the Modification of Commercial Bisphenol-A-Based Epoxy Resin Using Different Multifunctional Epoxy Systems. *Appl. Mech.* **2021**, *2*, 419–430. https://doi.org/10.3390/applmech2020023

Received: 27 April 2021
Accepted: 18 June 2021
Published: 21 June 2021

1. Introduction

Epoxy resins are widely used as matrices in composite materials for structural applications in the automotive and aerospace industries. This is due to their high strength and stiffness, as well as their excellent thermal and chemical resistance properties. The highly crosslinked networks that form, on the other hand, limit the network structure's mobility and induces brittleness in the cured system. The addition of soft fillers like rubber or thermoplastics to thermosets plasticize the structure, enhancing fracture toughness whilst lowering stiffness, strength, and glass transition temperature [1–3]. Similarly, Improvements in strength and modulus have also been reported where ceramic-based nanoparticles have been dispersed prior to curing [4–9]. A substantial amount of literature has been published claiming that both chemical modification and the addition of a secondary phase can alter the mechanical performance of epoxy polymers. The overarching trends from which are displayed in Table 1 [10–12].

With respect to reactant concentrations, the quantity of curing agent has been shown to alter the brittleness of epoxy polymers [13]. The antiplasticization phenomenon occurs when the hardener mass exceeds its stoichiometric ratio with epoxy, resulting in a rise in quasi-static modulus and a decrease in glass transition temperature, according to some researchers [14,15]. Mostovoy et al. [16] reported that ultimate tensile strength peaks at the stoichiometric ratio, while others suggest that ultimate strength is insensitive to curing agent concentration. Given the insufficient number of publications pertaining to strength alterations from chemical modification of epoxy systems, this research aims to elucidate this relationship. The main objective of this work was to compare blends of bisphenol-A-based epoxy and various multifunctional epoxies cured with anhydride hardener, with

regards to mechanical properties, fracture mechanics and thermal properties of the obtained modified systems.

Table 1. Influence of different modifiers on fracture-mechanical properties of epoxy-based micro/nanocomposites. (where "+" corresponds to a small increase and "−−" corresponds to a large reduction).

Modifiers	Fracture Toughness and Fracture Energy	Tensile Strength	Tensile Modulus
Reactive diluents	Increase +	Decrease −−	Decrease −−
Thermoplastics	Increase +	Decrease −−	Decrease −−
Rigid nanoparticles	Increase +	Increase +	Increase +
CTBN rubber	Increase ++	Decrease −−	Decrease −
CSR rubber	Increase +	Decrease −	Decrease −
Block copolymer	Increase ++	Decrease −	Decrease −

2. Materials

In the present work, CA144 liquid epoxy (Sika Chemicals, France) is used as a base matrix—see Figure 1a for skeletal formula. Alongside, CH141 (Figure 1b) acts as an anhydride-based hardener and CR144 is used as an accelerator (both from Sika Chemicals, France) [17]. The properties of the hardener and accelerator are listed in Table 2.

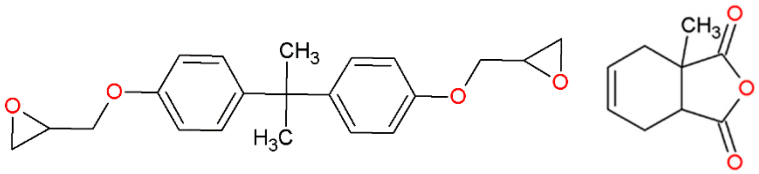

Figure 1. (**a**) Molecular structure of CA144 (diglycidyl ether of bisphenol–A) and (**b**) CH141 (tetrahydromethylphthalic anhydride).

Table 2. Properties of anhydride hardener, and accelerator used in the present work [17].

Properties	CA144	CH141	(CR144)
Equivalent weight (gm/eq.)	169	168	-
Density (g/cm^3)	1.16	1.20	1.03
Viscosity at 25 °C (Pa·s)	<12	<0.04	<0.01
Mixing ratio parts by weight	100	100	1.5
Gel time		100 min at 80 °C	

Araldite MY0610 (Figure 2a) is a particularly effective resin for a wide variety of formulating applications including composites, adhesives, laminating systems requiring high modulus, high hot-wet performance, and toughness. It is a high purity, low viscosity trifunctional distilled triglycidylether of meta-amino phenol [18]. Araldite MY0816 (Figure 2b) is a difunctional, low viscosity resin in which the flat rigid core facilitates multimolecular association, leading to highly compact networks. MY0816 possesses a strong aromatic character and low polarity backbone [19]. The developmental resin LME10169 (Figure 2c) is manufactured by Huntsman and supplied in the form of a colorless powder. LME10169 is a di-functional epoxy resin, with a large/bulky backbone providing structural rigidity via its high aromatic content. It is recommended for usage in structural composite matrices [20]. Table 3 lists the properties of the reference epoxy and all the multifunctional epoxy systems used in this work.

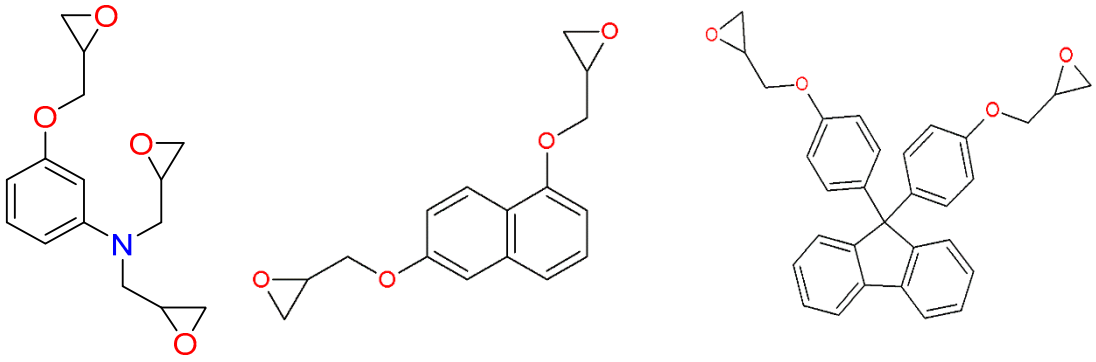

(**a**) MY0610 (**b**) MY0816 (**c**) LME10169

Figure 2. Molecular structure of (**a**) distilled triglycidylether of meta-amino phenol (Araldite MY0610), (**b**) 1,6-Naphthalene di epoxy (Araldite MY0816) and (**c**) fluorene di epoxy resin (LME10169).

Table 3. Properties of different epoxy systems used [17,18,21].

Property	CA144 (EP)	MY0610	MY0816	LME10169
Manufacturer	Sika	Huntsman	Huntsman	Huntsman
Viscosity @ 25 °C (Pa·s)	2.5–4.5	1.5–4.8	25–80	–
Epoxide equivalent weight (gm/eq.)	169	94–102	133–154	245–255
Functionality	2.1	3	2	2

3. Experimental Methods

This section covers the preparation of systems involving reference system CA144 epoxy and multifunctional epoxies such as fluorene di-epoxy (LME10169), 1,6-naphthalene di-epoxy (Araldite MY0816), and distilled triglycidylether of meta-amino phenol (Araldite MY0610). Each of the modifiers was stoichiometrically blended with reference CA144 epoxy resin in small amounts equating to 5 wt.%, 7 wt.% and 10 wt.%. Given the high viscosity of CR144 at room temperature, the component was heated to 60 °C for 10 min prior to being combined with a predetermined weight of the selected multifunctional epoxy. To maximize homogeneity, a mechanical mixer operating at 250 rpm for 20 min was used to blend the epoxy/multifunctional epoxies (see Figure 3). The mixture was subsequently cooled to 40 °C, into which the curing agent was added and mixed for an additional 15 min (at 250 rpm). The combined materials were then placed in a vacuum oven at 40 °C for 10 min to eliminate trapped air bubbles. The resultant blend was then cast into glass molds to produce a square-shaped sheet of 30 mm × 300 mm × 4 mm and into steel molds for compact tension (CT) specimens, respectively. The samples were then cured for 4 h at 80 °C and then post-cured for 8 h at 130 °C to complete the curing process. Once the cured plate was obtained, a CNC machine was used to cut dog-bone-shaped samples for tensile testing. In accordance with the Biresin CR144 technical datasheet, a post-cure temperature approximately 10 °C below the recommended glass transition temperature was chosen, where an extended dwell period of 4 h promoted maximum conversion [17].

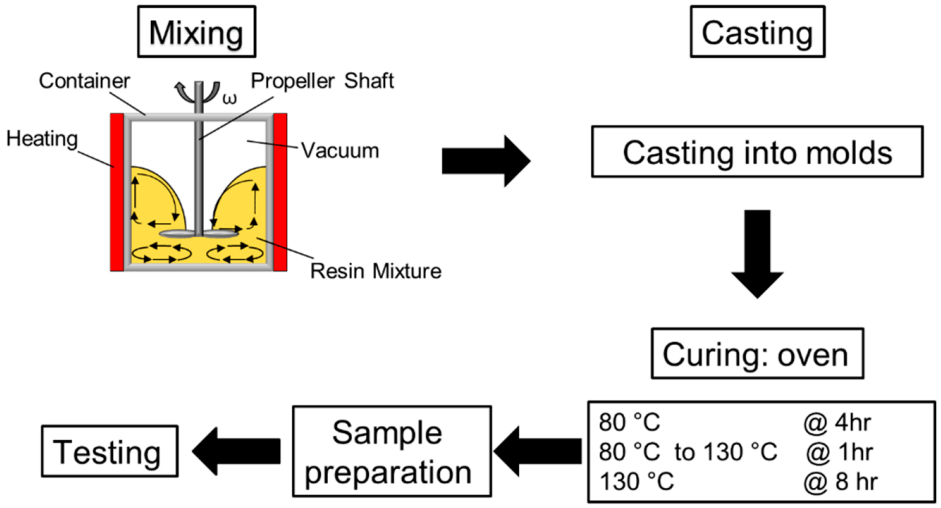

Figure 3. Schematic diagram of sample preparation.

3.1. Tensile Tests

Tensile tests were conducted at 23 °C, 60 °C, and 80 °C on a universal testing machine with a 10 kN load cell (Instron Inc., 5500R, Norwood, MA, USA) in accordance with DIN EN ISO 527-2 [22]. Dog-bone-shaped (ISO 572-2 type 1B) samples with gauge lengths of 50 mm, 10 mm widths, and thicknesses of 4 mm were used- see Figure 4a,b. The distance between the clamped surfaces was 115 mm and the testing speed was 2 mm/min. A precision sensor-arm extensometer was utilized to determine the specimen strain. From the resulting stress–strain diagrams, the tensile modulus was determined from the slope of the curve between 0.05% and 0.25% of the total strain. The tensile strength was determined from the material's maximum sustained stress. For high-temperature testing, a temperature cabinet was attached to provide a consistent prescribed temperature at the clamping and specimen locations. For all elevated temperature tests, specimens were kept in the chamber for a minimum of 2 h, to ensure that samples were evenly heated throughout. As required, a minimum of five samples was tested for each formulation [22].

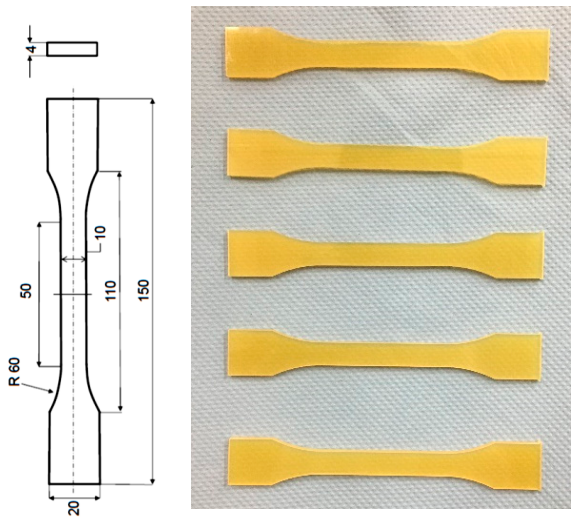

(**a**) (**b**)

Figure 4. (**a**) EN ISO 527-2 type 1B geometry for the tensile test specimens. All dimensions are in mm. (**b**) Photograph of epoxy-based dog-bone specimens used for tensile testing.

3.2. Differential Scanning Calorimetry (DSC)

DSC was performed on a Q100 (TA Instruments, New Castle, DE, USA) system to measure heat-flux against temperature and time, from which glass transition temperatures (T_g) could be inferred. To begin, the cured sample material was weighed (approximately 7–13 mg) and put in a crucible, which was then sealed with a lid using a crucible sealing press. Along with an empty reference crucible, the sample was heated from room temperature to 200 °C using a heating rate of 10 °C/min.

3.3. Dynamic Mechanical Thermal Analysis (DMA)

In the present study, the storage modulus, loss modulus, and tan δ of all bulk samples were measured by dynamic mechanical thermal analysis using a DMA machine from TA Instruments (New Castle, DE, USA). Analyses were performed in 3-point bending mode at 1 H_z, on 60 mm × 10 mm × 4 mm specimens. Again, the glass transition temperature, T_g of the bulk epoxy samples were determined; in this case, using the peak value of tan δ [23]. The peak δ method was selected over derivative approaches for simplicity, and in accordance with the DMA machine manufacturer recommendations [24]. The temperature program was set as −120 °C to 200 °C with a heating rate of 2 °C/min.

3.4. Fracture Toughness Tests

The intrinsic fracture toughness of brittle solids can be measured using linear elastic fracture mechanics (LEFM) [25]. LEFM provides details about the initiation of cracks in cured epoxy samples regardless of specimen geometry. At 23 °C, the plane strain fracture toughness (K_{Ic}) of the composites was measured using compact tension (CT) samples under tensile loading conditions according to ISO 13586 and a strain rate of 0.2 mm/min [26]. The specimens' thickness B and width W were selected as 6 mm and 36 mm, respectively. A minimum of five specimens was tested for each system and samples were tested on a universal testing unit (Instron Inc., 5500R, Norwood, MA, USA). A sharp crack of length a_o ($0.45*W \leq a_o \leq 0.55*W$), where W is the distance between the axis of load application and the end of the sample, was generated by the controlled impact of a new scalpel blade to produce the necessary critical stress condition in the material. The form and dimensions of the compact tension samples used for fracture testing are shown in Figure 5.

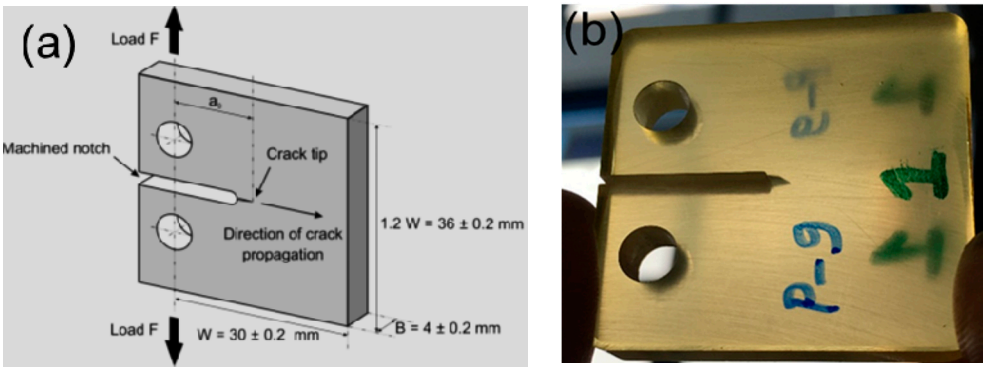

Figure 5. (**a**) Geometry of Compact Tension samples used for fracture testing in mode-I condition. (**b**) Photograph of compact tension sample prepared with artificial sharp crack.

Previous research [27] indicates that a scalpel blade can be effectively utilized for introducing an initial crack in rubber toughened and pure epoxy resins. The linear elastic fracture mechanics approach assumes that the plastically deformed region in front of the crack tip is small in comparison to the total crack length. Careful tapping results in a straight crack front, a compact pre-crack tip radius and minimal residual stresses around the crack tip. As a result, the requirements for using the linear elastic method are met, further ensuring that the experimental results provide reasonable fracture toughness values for the materials.

The fracture toughness K_{Ic} was then calculated with Equation (1),

$$K_{Ic} = \frac{F}{B\sqrt{W}}.f(a_o/W) \quad (1)$$

where F is the maximum force observed in the load–displacement curve, B is the sample width, W is the distance between the axis of load application and the end of the sample, and a_o is the initial crack length for calculating $\alpha = a_o/W$. The mapping $f(a_o/W)$ is the geometry function for the compact tension sample, which is expressed by (Equation (2)) [26].

$$f(\alpha) = \frac{(2+\alpha)}{(1-\alpha)^{3/2}}.\left(0.866 + 4.64\alpha - 13.32\alpha^2 + 14.72\alpha^3 - 5.60\alpha^4\right) \quad (2)$$

The critical energy release rate G_{Ic} can then be calculated (Equation (3)) using the critical stress intensity factor K_{Ic}, the elastic modulus E_t, and Poisson's ratio v (~0.35):

$$G_{Ic} = \frac{K_{Ic}^2(1-v^2)}{E_t} \quad (3)$$

3.5. Scanning Electron Microscopy

Scanning electron microscopy (SEM) was used as a means of qualitatively assessing the failure behavior of tensile and compact tension samples. SEM specimens were prepared with a 40-nm sputter coating of gold to enhance surface conductivity and imaged at 5 kV on a JEOL JSM series instrument. Sputtering was applied to the fractured surfaces of both the tensile and compact tension samples.

4. Results and Discussion

4.1. Tensile and Fracture Properties

Table 4 lists the properties of the reference system and modified systems that were manufactured by blending the three multifunctional resins at 5 wt.%, 7 wt.% and 10 wt.%. For all modified epoxy systems, the maximum tensile strength and modulus were obtained at 10 wt.%—see Figure 6 for the representative stress–strain response of the 10 wt.% modified systems. It can be observed that EP_10MY0610 system exhibited superior performance in terms of tensile strength, tensile modulus, and glass transition temperature, when compared against the reference system. The greater degree of crosslinking and increased length, contribute to the increased tensile strength over the reference epoxy resin. This performance improvement may also be partly attributed to a degree of increased polymer chain entanglement. Another possible reason for higher strength and modulus comes from the introduction of additional rigid, polar groups with higher functionality in comparison to the DGEBA system, which ultimately increases the crosslink density within the system. The EP_10MY0610 was selected for further testing and is discussed more extensively in the following section. From this part onwards, EP_10MY0610 is simply denoted as MEP, whilst the reference system remains denoted by EP.

Table 4. Mechanical, thermal, and fracture properties of the reference system and modified systems.

Systems	E_t (MPa)	σ_m (MPa)	ε_m (%)	T_g (°C)	K_{Ic} (MPa·m$^{1/2}$)
EP	3450 (±40)	90 (±0.66)	5.7 (±0.01)	141	0.59 (±0.10)
EP_5LME	3470 (±34)	91 (±0.95)	5.7 (±0.04)	144	0.62 (±0.05)
EP_7LME	3440 (±10)	92 (±0.28)	5.7 (±0.08)	143	0.58 (±0.12)
EP_10LME	3520 (±30)	100 (±1.0)	5.8 (±0.03)	144	0.66 (±0.06)
EP_5MY0816	3500 (±65)	98 (±0.58)	5.8 (±0.06)	143	0.60 (±0.07)
EP_7MY0816	3330 (±18)	95 (±0.50)	5.8 (±0.02)	144	0.55 (±0.05)

Table 4. *Cont.*

Systems	E_t (MPa)	σ_m (MPa)	ε_m (%)	T_g (°C)	K_{Ic} (MPa·m$^{1/2}$)
EP_10MY0816	3510 (±36)	100 (±0.65)	5.8 (±0.02)	144	0.65 (±0.08)
EP_5MY0610	3460 (±77)	94 (±0.66)	5.7 (±0.04)	143	0.56 (±0.09)
EP_7MY0610	3440 (±45)	97 (±0.66)	5.8 (±0.06)	145	0.60 (±0.16)
EP_10MY0610	3580 (±78)	102 (±0.66)	5.8 (±0.01)	148	0.64 (±0.11)

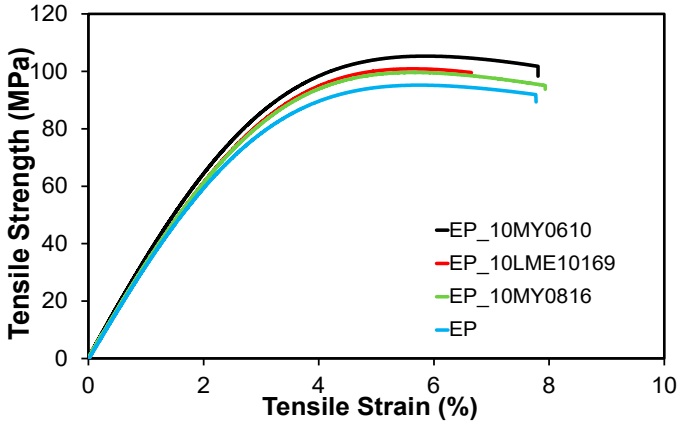

Figure 6. Representative stress–strain diagram for reference (EP) and 10 wt.% modified systems. (all tests were performed at 23 °C).

Fractographs from tensile testing at room temperature are shown in Figure 7a,b. The crack initiation and crack propagation zones are the two discrete and separate areas of the fracture surface. Observing the SEM images, the former appears grey and is differentiated by a comparatively smooth region, as well as various river marks that indicate fracture propagation on somewhat different planes. The crack propagation zone surrounds the crack initiation zone and is characterized by an extremely rough surface with hackles or ribbons radiating radially from the initiation point, and multiple fracture stages in between. The smooth area generally refers to the sub-critical crack development zone or the zone where the crack is accelerating, while the rough area refers to the rapid fracture zone, which is generated owing to the main crack's extensive branching. Similarly, SEM fractographs also provide valuable insight into the fracture behaviour of the modified epoxy systems—see Figure 7c,d. The fracture surface of the MEP specimens (along with the other modified systems) appears smooth with no large features available for comparison with the fracture surface of the EP reference system.

4.2. Thermal and Viscoelastic Properties

For each modified system, T_g values obtained from DSC measurements are listed in Table 4. It is clear that all of the modified systems have either the same or higher glass transition temperatures than the reference system. For the selected modified system (MEP), the T_g was 148 °C (from DSC), and for the same system, it was also confirmed by the tan δ vs temperature (DMA) graph shown in Figure 8, the storage modulus vs. temperature curve shifts towards the right and is larger over the same temperature range, when compared to the EP system (above 125 °C). This indicates that the T_g of the modified system is higher than the reference anhydride system. Similarly, the tan δ curve displays the same tendency for the modified system to shift right, highlighting its larger T_g and reduced damping factor (when compared with the reference anhydride system).

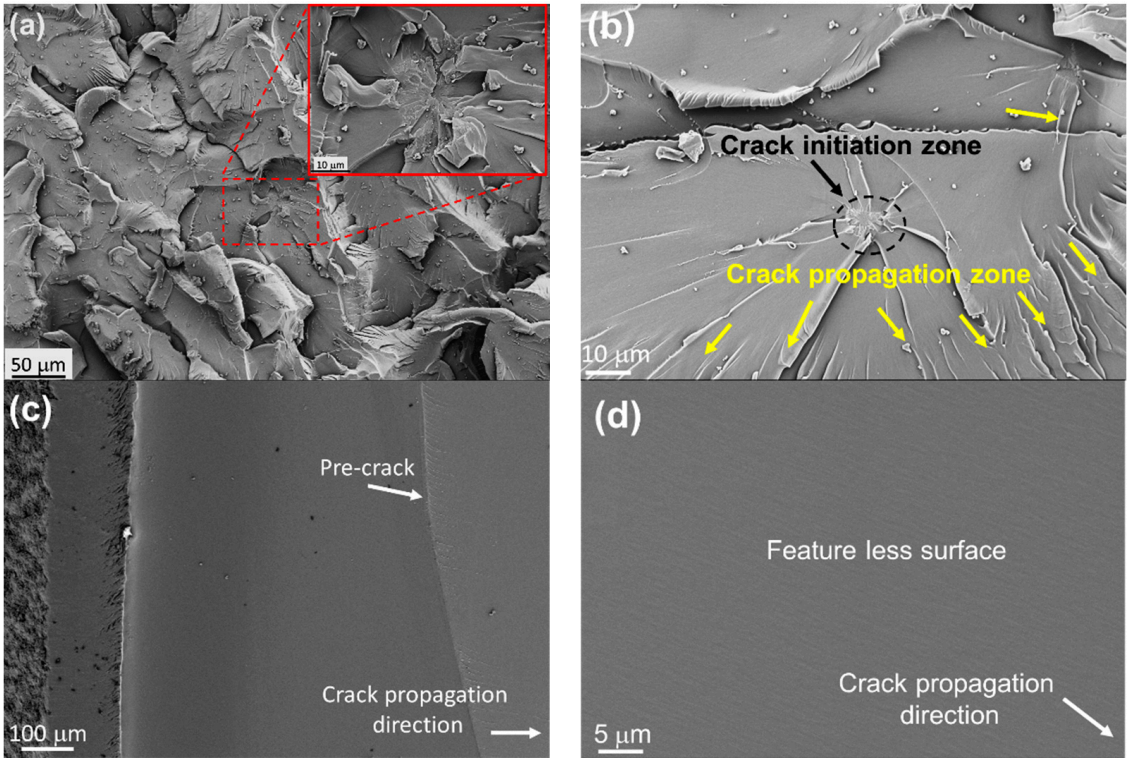

Figure 7. High Magnification SEM fractographs of representative MEP (**a**,**b**) tensile test specimen fracture surfaces and (**c**,**d**) compact tension specimen fracture surfaces, at room temperature.

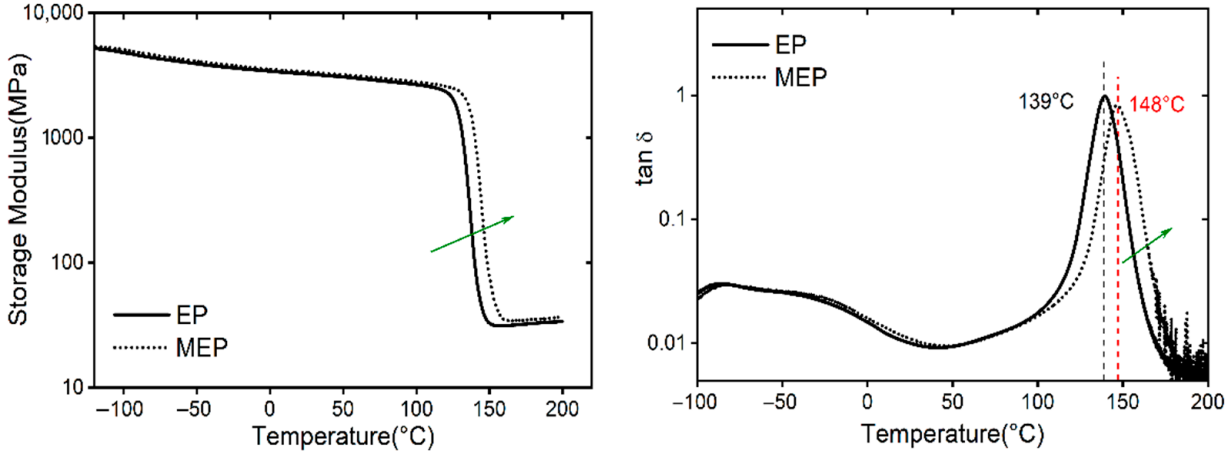

Figure 8. Comparison of the DMA curves for the reference epoxy (EP) and the modified epoxy system (MEP). tan vs. temperature (**right**) and storage modulus vs. temperature (**left**).

Figure 9 depicts the effect of frequency on the tan δ vs. temperature and elastic modulus vs. temperature curves. Both plots demonstrate that as frequency rises, the system's glass transition temperature also increases. However, for the rest of the modified systems, a standard frequency of 1 H_z was selected.

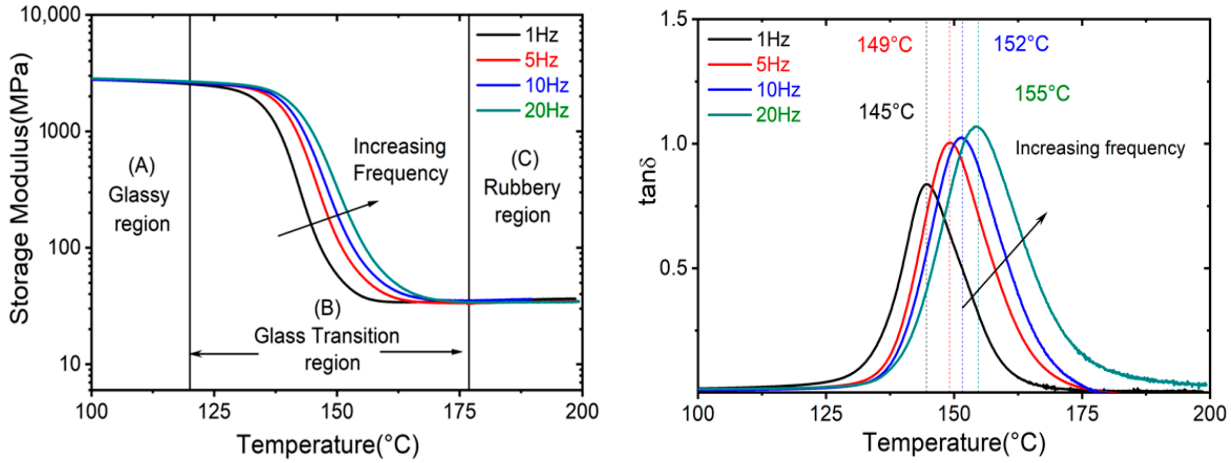

Figure 9. Effect of varying frequencies on the MEP system. Storage modulus vs. temperature curve (**left**) and tan δ vs. temperature (**right**).

4.3. Effect of Strain Rate on Tensile Properties

In observing Figure 10, it is apparent that increasing the strain rate resulted in an increase in tensile strength for MEP specimens. These plots were obtained via tensile tests carried out at a temperature of 23 °C. Although the strain rate has a significant impact on maximum tensile stress at temperatures below T_g, Young's modulus remains nearly constant for all strain rates. Furthermore, no such behaviour could be observed for the tensile strain magnitude, since yield strength is generally only affected by pressure, temperature, and strain rate [28,29].

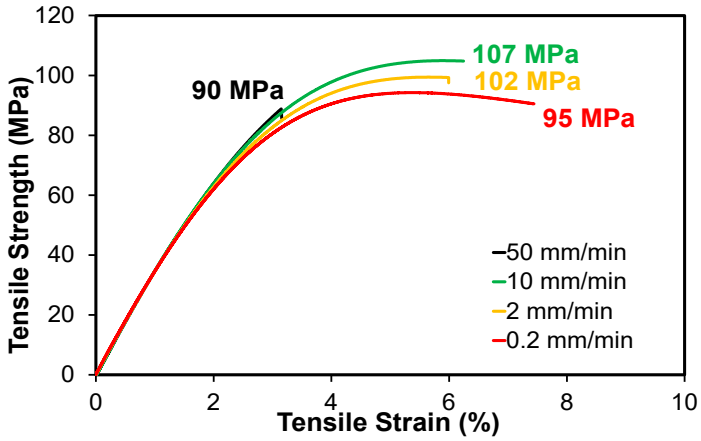

Figure 10. Representative stress–strain curves for the modified system (MEP) with different stain rates.

4.4. Effect of Temperature on Tensile Properties

Figure 11 shows how temperature affects the tensile strength of EP and MEP systems. The increase in ductility is accompanied by a decrease in tensile modulus and ultimate tensile strength as the temperature rises. As the temperature approached the T_g region at 80 °C, the decrease in tensile strength became more pronounced, indicating that the epoxy/hardener system was transitioning from a glassy to a rubbery state. It is also possible to deduce that as the temperature rises, the epoxy becomes more ductile, resulting in a higher strain-to-failure ratio. With the rise in temperature, the mobility of the polymer chains in the epoxy hardener system increases, resulting in a higher strain to failure. At temperatures of 23 °C, 60 °C, and 80 °C, Figure 11 shows that the (MEP) system outperforms the (EP) system.

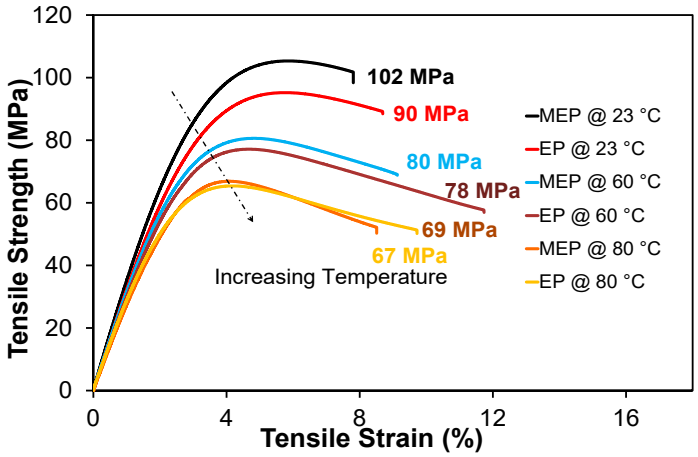

Figure 11. Effect of temperature on the stress–strain curve for the anhydride-based reference (EP) and modified epoxy (MEP) systems. At 23 °C, 60 °C, and 80 °C.

4.5. Effect of Moisture on Tensile Properties

A small extra piece of work was performed for water ageing studies. The dog-bone samples of the anhydride-based reference (EP) and modified epoxy (MEP) systems were submerged in de-ionized water at 25 °C for 1 week, then removed and tensile testing was performed. For the EP and MEP systems, weight increases of 0.15% and 0.13%, respectively, were calculated. As seen in Figure 12, water acts as a plasticizer, reducing mechanical properties such as strength and moduli [30,31]. In both dry and wet conditions, it can be shown that the modified system (MEP) has superior properties when compared with the reference system (EP).

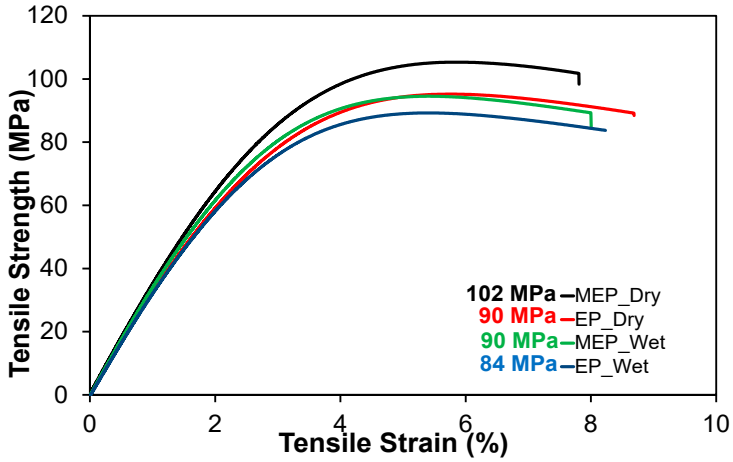

Figure 12. Representative stress–strain curves for anhydride-based reference (EP) and modified (MEP) epoxy systems. In dry and wet environments.

5. Conclusions

The findings presented here show how di- and tri-functional epoxy copolymers can be used to improve the tensile strength of an aromatic DGEBA/anhydride epoxy system. The tensile modulus and tensile strength showed slight increases of 4% and 14%, respectively while the sample ductility remained the same for the MEP system. The introduction of different multifunctional epoxy into different epoxy resins increases the storage modulus at the glassy region and shifts the curve towards higher temperatures, indicating an increased glass transition temperature in the modified epoxy system (MEP). The plane–strain fracture toughness almost remains the same with the addition of different multifunctional epoxy systems. It can be concluded that for mechanical properties such as Young's modulus and

tensile strength, modified epoxy systems containing 10 wt.% multifunctional epoxy were the highest performing. Further, it was revealed that these properties are temperature, strain rate- and moisture-dependent. Tensile strength and modulus of elasticity increased by increasing the strain rate at room temperature, while ductility instead decreased. Tensile strength and modulus of elasticity decreased upon increasing the temperature, while ductility increased. Compared to the reference system (EP), the selected modified system (MEP) exhibits superior properties at various temperatures, under both dry and wet environmental conditions.

Author Contributions: Conceptualization, A.B.; methodology, A.B.; formal analysis, A.B.; investigation, A.B., J.R.D.; writing—original draft preparation, A.B.; writing—review and editing, A.B., C.R. and J.R.D. All authors have read and agreed to the published version of the manuscript.

Funding: This research received no external funding.

Institutional Review Board Statement: Not applicable.

Informed Consent Statement: Not applicable.

Acknowledgments: Authors like to thank Sika Chemical, France, and Huntsman Materials, Switzerland for the provision of the materials. Furthermore, the authors thank Danijela Stankovic for fruitful discussions.

Conflicts of Interest: The authors declare no conflict of interest.

References

1. Klingler, A.; Bajpai, A.; Wetzel, B. The effect of block copolymer and core-shell rubber hybrid toughening on morphology and fracture of epoxy-based fibre reinforced composites. *Eng. Fract. Mech.* **2018**, *203*, 81–101. [CrossRef]
2. Bajpai, A.; Wetzel, B.; Friedrich, K. High strength epoxy system modified with soft block copolymer and stiff core-shell rubber nanoparticles. *Express Polym. Lett.* **2020**, *14*, 384–399. [CrossRef]
3. Bajpai, A.; Wetzel, B. Effect of different types of block copolymers on morphology, mechanical properties, and fracture mechanisms of bisphenol-F based epoxy system. *J. Compos. Sci.* **2019**, *3*, 68. [CrossRef]
4. Bajpai, A.; Carlotti, S. The Effect of Hybridized Carbon Nanotubes, Silica Nanoparticles, and Core-Shell Rubber on Tensile, Fracture Mechanics and Electrical Properties of Epoxy Nanocomposites. *Nanomaterials* **2019**, *9*, 1057. [CrossRef]
5. Bajpai, A.; Alapati, A.K.; Klingler, A.; Wetzel, B. Tensile properties, fracture mechanics properties and toughening mechanisms of epoxy systems modified with soft block copolymers, rigid TiO2 nanoparticles and their hybrids. *J. Compos. Sci.* **2018**, *2*, 72. [CrossRef]
6. Bajpai, A.; Alapati, K.; Wetzel, B. Toughening and mechanical properties of epoxy modified with block co-polymers and MWCNTs. *Procedia Struct. Integr.* **2016**, *2*, 104–111. [CrossRef]
7. Bajpai, A.; Martin, R.; Faria, H.; Ibarboure, E.; Carlotti, S. Epoxy based hybrid nanocomposites: Fracture mechanisms, tensile properties and electrical properties. *Mater. Today Proc.* **2021**, *34*, 210–216. [CrossRef]
8. Hsieh, T.H.; Kinloch, A.J.; Masania, K.; Taylor, A.C.; Sprenger, S. The mechanisms and mechanics of the toughening of epoxy polymers modified with silica nanoparticles. *Polymer* **2010**, *51*, 6284–6294. [CrossRef]
9. Sprenger, S. Nanosilica-toughened epoxy resins. *Polymers* **2020**, *12*, 1777. [CrossRef]
10. Unnikrishnan, K.P.; Thachil, E.T. Hybrid polymer networks of epoxy resin and substituted phenolic novolacs. *Int. J. Polym. Mater.* **2006**, *55*, 563–576. [CrossRef]
11. Unnikrishnan, K.P.; Thachil, E.T. Studies on the Modification of Commercial Epoxy Resin using Cardanol-Based Phenolic Resins. *J. Elastomers Plast.* **2008**, *40*, 271–286. [CrossRef]
12. Downey, M.A.; Drzal, L.T. Toughening of aromatic epoxy via aliphatic epoxy copolymers. *Polymer* **2014**, *55*, 6658–6663. [CrossRef]
13. Khalina, M.; Beheshty, M.H.; Salimi, A. Preparation and characterization of DGEBA/EPN epoxy blends with improved fracture toughness. *Chin. J. Polym. Sci.* **2018**, *36*, 632–640. [CrossRef]
14. Bellenger, V.; Dhaoui, W.; Verdu, J.; Lacabanne, J.B.C. Internal antiplasticization in diglycidyl ether of bisphenol A diamino diphenyl methane non-stoichiometric epoxy networks. *Polym. Eng. Sci.* **1990**, *30*, 321–325. [CrossRef]
15. Mafi, E.R.; Ebrahimi, M.; Moghbeli, M.R. Effect of matrix crosslink density, varied by stoichiometry and resin molecular weight, on fracture behavior of epoxy resins. *J. Polym. Eng.* **2009**, *29*, 293–308. [CrossRef]
16. Mostovoy, S.; Ripling, E.J. Fracture toughness of an epoxy system. *J. Appl. Polym. Sci.* **1966**, *10*, 1351–1371. [CrossRef]
17. Sika Deutschland GmbH. Biresin®CR144 Product Data Sheet. 2020. Available online: https://industry.sika.com/content/dam/dms/global-industry/m/Biresin-CR144-Anhydrid-New.pdf (accessed on 1 June 2021).
18. Huntsman. *Technical Data Sheet for Araldite MY 0610 Trifunctional Resin*; Huntsman Advance Materials GmbH: Basel, Switzerland, 2015.
19. Huntsman. *Technical Data Sheet for Araldite MY 0816*; Huntsman Advance Materials GmbH: Basel, Switzerland, 2015.

20. Huntsman. *Technical Data Sheet for Developmental Resin LME10169*; Huntsman Advance Materials GmbH: Basel, Switzerland, 2015.
21. Huntsman. Advance Material Raising Performance with Building Blocks. 2012. Available online: http://www.huntsman.com/advanced_materials/Media%20Library/global/files/EUR_HL_Components_Raising%20performance%20with%20Building%20blocks.pdf (accessed on 10 April 2021).
22. DIN-EN-ISO-527-1. *General Principles for the Determination of Tensile Properties*; DIN Deutsches Institut für Normung: Berlin, Germany, 1996.
23. ISO 6721-11:2019 Plastics. *Determination of Dynamic Mechanical Properties—Part 11: Glass Transition Temperature*; ISO (The International Organization for Standardization): Berlin, Germany, 2019.
24. TA Instruments. Measurement of Glass Transition Temperatures by Dynamic Mechanical Analysis and Rheology (RH100). Available online: https://www.tainstruments.com/pdf/literature/RH100.pdf (accessed on 3 May 2021).
25. Kinloch, A.J.; Young, R.J. *Fracture Behaviour of Polymers*; Elsevier Applied Science: New York, NY, USA, 1983.
26. ISO 13586:2000(E). *Plastics—Determination of Fracture Toughness (GIc and KIc)—Linear Elastic Fracture Mechanics (LEFM) Approach*; ISO (The International Organization for Standardization): Gevena, Switzerland, 2018.
27. Xiao, K.; Ye, L.; Kwok, Y.S. Effects of pre-cracking methods on fracture behaviour of an Araldite-F epoxy and its rubber-modified systems. *J. Mater. Sci.* **1998**, *33*, 2831–2836. [CrossRef]
28. Yamini, S.; Young, R.J. The mechanical properties of epoxy resins. *J. Mater. Sci.* **1980**, *15*, 1814–1822. [CrossRef]
29. Cook, W.D.; Mayr, A.E.; Edward, G.H. Yielding behaviour in model epoxy thermosets—II. Temperature dependence. *Polymer* **1998**, *39*, 3725–3733. [CrossRef]
30. Wylde, J.; Spelt, J. Measurement of adhesive joint fracture properties as a function of environmental degradation. *Int. J. Adhes. Adhes.* **1998**, *18*, 237–246. [CrossRef]
31. Wahab, M.; Crocombe, A.; Beevers, A.; Ebtehaj, K. Coupled stress diffusion analysis for durability study in adhesively bonded joints. *Int. J. Adhes. Adhes.* **2002**, *22*, 61–73. [CrossRef]